International Journal of Solids and Structures 46 (2009) 2757–2764

Contents lists available at ScienceDirect

International Journal of Solids and Structures

journal homepage: www.elsevier.com/locate/ijsolstr

A new Kirchhoff plate model based on a modified couple stress theory

G.C. Tsiatas *

Institute of Structural Analysis, School of Civil Engineering, National Technical University of Athens, Zografou Campus, GR-15773 Athens, Greece

ARTICLE INFO

Article history:
Received 12 January 2009
Received in revised form 18 February 2009
Available online 20 March 2009

Keywords:
Couple stress elasticity
Gradient elasticity
Kirchhoff plate
Method of fundamental solutions
Meshless methods

ABSTRACT

In this paper a new Kirchhoff plate model is developed for the static analysis of isotropic micro-plates with arbitrary shape based on a modified couple stress theory containing only one material length scale parameter which can capture the size effect. The proposed model is capable of handling plates with complex geometries and boundary conditions. From a detailed variational procedure the governing equilibrium equation of the micro-plate and the most general boundary conditions are derived, in terms of the deflection, using the principle of minimum potential energy. The resulting boundary value problem is of the fourth order (instead of existing gradient theories which is of the sixth order) and it is solved using the Method of Fundamental Solutions (MFS) which is a boundary-type meshless method. Several plates of various shapes, aspect and Poisson's ratios are analyzed to illustrate the applicability of the developed micro-plate model and to reveal the differences between the current model and the classical plate model. Moreover, useful conclusions are drawn from the micron-scale response of this new Kirchhoff plate model.

1. Introduction

The behavior of micron-scale structures has been proven experimentally to be size dependent. Therefore, the classical continuum theory is inadequate to predict their response and the utilization of strain gradient (higher order) theories containing internal material length scale parameters is inevitable. For a literature review of the afore-mentioned theories can be found in the recent works of Vardoulakis and Sulem (1995); Exadaktylos and Vardoulakis (2001) and Tsepoura et al. (2002). Although, the strain gradient theories encounter the physical problem in its generality, they contain additional constants – besides the Lamé constants - which are difficult to determine even in their simplified form containing only two additional constants (Lam et al., 2003). Thus, gradient elasticity theories of only one additional material constant have been developed.

Altan and Aifantis (1992) suggested a simplified strain gradient model with only one strain gradient coefficient of length squared dimension which has been used by many investigators (e.g., Askes and Aifantis, 2002; Lazopoulos, 2004; Papargyri-Beskou and Beskos, 2008). A variational formulation of this simplified gradient elasticity theory has been presented by Gao and Park (2007) determining simultaneously both the equilibrium equations and the complete boundary conditions for the first time.

Yang et al. (2002) – modifying the classical couple stress theory (e.g. Mindlin, 1964; Koiter, 1964) – proposed a modified couple stress model in which only one material length parameter is needed to capture the size effect. This simplified couple stress theory is based on an additional equilibrium relation which force the couple stress tensor to be symmetric. So far has been developed for the static bending (Park and Gao, 2006) and free vibration (Kong et al., 2008) problems of a Bernoulli-Euler beam and for the static bending and free vibration problems of a Timoshenko beam (Ma et al., 2008). Moreover, Park and Gao (2008) solved analytically a simple shear problem after the derivation of the boundary conditions and the displacement form of the theory.

The work that has been done on the analysis of micro-plates is limited only to publications of linear and nonlinear plate models based on the simplified strain gradient model with one internal parameter introduced by Altan and Aifantis (1992). More specifically, Lazopoulos (2004) developed a strain gradient geometrically nonlinear plate model modifying Von Karman's nonlinear equations. This model was implemented in the study of the localized buckling of a long plate under uniaxial in-plane compression and small lateral loading, using the multiple scales perturbation method. Papargyri-Beskou and Beskos (2008) derived explicitly the governing equation of motion of gradient elastic flexural Kirchhoff plates, including the effect of in-plane constant forces on bending. In their work three boundary value problems were investigated (using the double Fourier series solution) dealing with static, stability and dynamic analysis of a rectangular simply supported gradient elastic flexural plate. However, the main drawback of the above plate models is that the presence of the microstructural effect raises the order of the resulting partial differential equation form four (classical case) to six (gradient case). As well as the classical boundary conditions are supplemented by additional (non-classical) ones containing higher order traction and higher

* Tel.: +30 2107721627; fax: +30 2107721655.
E-mail address: gtsiatas@gmail.com

0020-7683/$ - see front matter © 2009 Elsevier Ltd. All rights reserved.
doi:10.1016/j.ijsolstr.2009.03.004

order moments. Hence, the employed analytical solutions are restricted only to simple geometric shapes.

In this paper a new Kirchhoff plate model is developed for the static analysis of isotropic micro-plates with arbitrary shape based on the simplified couple stress theory of Yang et al. (2002) containing only one material length scale parameter which can capture the size effect. The proposed model is capable of handling plates with complex geometries and boundary conditions. To the author knowledge publications on the solution of the particular problem have not been reported in literature. The rest of paper is organized as follows. In Section 2 the total potential energy and its first variation of a three-dimensional body in rectangular coordinates are presented according to the modified couple stress theory. Using the minimum potential energy principle the governing equilibrium equation together with the pertinent boundary conditions in terms of the deflection are derived in their most general form, including elastic support or restraint, in Section 3. The resulting boundary value problem of the micro-plate is of the fourth order and it is solved using the Method of Fundamental Solutions (MFS) in Section 4. Several plates of various shapes, aspect and Poisson's ratios are analyzed in Section 5 to illustrate the developed micro-plate model and to reveal the differences between the current model and the classical plate model. Finally, a summary of conclusions is given in Section 6.

2. Modified coupled stress theory

In the modified couple stress theory of Yang et al. (2002), the strain energy density in rectangular coordinates of a three-dimensional body occupying a volume V bounded by the surface Ω is given as

$$U = \frac{1}{2}\int_V (\sigma_{ij}\varepsilon_{ij} + m_{ij}\chi_{ij})dV \tag{1}$$

where

$$\varepsilon_{ij} = \frac{1}{2}(u_{i,j} + u_{j,i}) \tag{2}$$

$$\chi_{ij} = \frac{1}{2}(\theta_{i,j} + \theta_{j,i}) \tag{3}$$

are the strain tensor and the symmetric part of the curvature tensor, respectively, u_i is the displacement vector and θ_i is the rotation vector defined as (Yang et al., 2002)

$$\theta_i = \frac{1}{2}e_{ijk}u_{k,j} \tag{4}$$

where e_{ijk} is the permutation symbol. In what it follows, unless otherwise stated, the Greek indices take the values 1, 2, while the Latin indices take the values 1, 2, 3. Moreover, σ_{ij} is the stress tensor and m_{ij} is the deviatoric part of the couple stress tensor given as

$$\sigma_{ij} = \lambda\varepsilon_{kk}\delta_{ij} + 2\mu\varepsilon_{ij} \tag{5}$$

$$m_{ij} = 2\mu l^2\chi_{ij} \tag{6}$$

where, λ and μ are the Lamé constants, δ_{ij} is the Kronecker delta and l is a material length scale parameter. From Eq. (3) it can be noted that the curvature tensor χ_{ij} is symmetric and consequently from Eq. (6) the couple stress tensor m_{ij} is also symmetric. That is, only the symmetric part of displacement gradient and the symmetric part of rotation gradient contribute to the deformation energy (Yang et al., 2002) which is different from that in the classical couple stress theory (e.g. Mindlin, 1964; Koiter, 1964).

Following Yang et al. (2002) and Park and Gao (2008), the work produced by the external forces is

$$W = \int_V (b_i u_i + c_i\theta_i)dV + \int_\Omega (t_i u_i + s_i\theta_i)d\Omega \tag{7}$$

where b_i, c_i, t_i, and s_i are the body force, body couple, traction and surface couple, respectively. Hence, the total potential energy of the deformable body using Eqs. (1) and (7) is written as

$$\Pi = U - W = \frac{1}{2}\int_V (\sigma_{ij}\varepsilon_{ij} + m_{ij}\chi_{ij})dV - \int_V (b_i u_i + c_i\theta_i)dV - \int_\Omega (t_i u_i + s_i\theta_i)d\Omega \tag{8}$$

and its first variation gives

$$\delta\Pi = \int_V (\sigma_{ij}\delta\varepsilon_{ij} + m_{ij}\delta\chi_{ij})dV - \int_V (b_i\delta u_i + c_i\delta\theta_i)dV - \int_\Omega (t_i\delta u_i + s_i\delta\theta_i)d\Omega \tag{9}$$

3. Governing equation and pertinent boundary conditions of micro-plates

Consider an initially flat thin elastic plate of thickness h consisting of homogeneous linearly elastic material occupying the two-dimensional domain Ω of arbitrary shape in the x, y plane bounded by the curve Γ which may be piecewise smooth, i.e. it may have a finite number of corners (see Fig. 1). The plate is bending under the combined action of the distributed transverse load $q(x, y)$, the edge moment $\widetilde{M}_{nn}$ and the edge force $\widetilde{V}_n$ producing a three dimensional deformation state including the transverse deflection $w(x, y)$ and the in plane displacements $u_\alpha(x, y, z)$ which in the absence of in plane forces are written as (Timoshenko and Woinowsky-Krieger, 1959)

$$u_\alpha(x, y, z) = -zw_{,\alpha} \tag{10}$$

Taking into account Eqs. (10), (4) and that

$$w_{,1} \equiv w_{,x}, \quad w_{,2} \equiv w_{,y} \tag{11}$$

the displacement and rotation vectors of the micro-plate become, respectively,

$$\mathbf{u} = -zw_{,x}\,\mathbf{e}_1 - zw_{,y}\,\mathbf{e}_2 + w\mathbf{e}_3 \tag{12}$$

$$\boldsymbol{\theta} = w_{,y}\,\mathbf{e}_1 - w_{,x}\,\mathbf{e}_2 \tag{13}$$

Substituting Eqs. (12) and (13) into Eqs. (2) and (3) the nonzero components of the strain and curvature tensor are written as

$$\varepsilon_x \equiv \varepsilon_{11} = -zw_{,xx}, \quad \varepsilon_y \equiv \varepsilon_{22} = -zw_{,yy}, \quad \gamma_{xy} \equiv 2\varepsilon_{12} = -2zw_{,xy} \tag{14a,b,c}$$

$$\chi_x \equiv \chi_{11} = w_{,xy}, \quad \chi_y \equiv \chi_{22} = -w_{,xy}, \quad \chi_{xy} \equiv \chi_{12} = \frac{1}{2}(w_{,yy} - w_{,xx}) \tag{15a,b,c}$$

respectively.

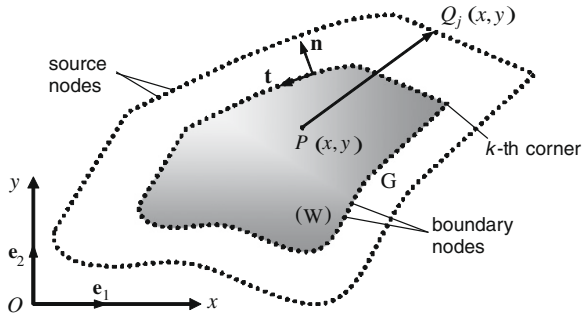

Fig. 1. Plate geometry and distribution of the boundary and source nodes.

The two dimensional state of stress is described by the stress (5) and couple stress (6) tensors which, after the appropriate replacement of the Lamé constants by the modulus of elasticity E and the Poisson's ratio ν (Timoshenko and Goodier, 1970), take the following form

$$\sigma_{\alpha\beta} = \frac{E}{1-\nu^2}[\nu\varepsilon_{\kappa\kappa}\delta_{\alpha\beta} + (1-\nu)\varepsilon_{\alpha\beta}] \tag{16}$$

$$m_{\alpha\beta} = 2Gl^2\chi_{\alpha\beta} \tag{17}$$

where $G = E/2(1+\nu)$ is the shear modulus.

We define, respectively, the bending moment and the couple moment tensors as

$$M_{\alpha\beta} = \int_{-h/2}^{h/2} \sigma_{\alpha\beta} z dz \tag{18}$$

$$Y_{\alpha\beta} = \int_{-h/2}^{h/2} m_{\alpha\beta} dz \tag{19}$$

which in terms of their components are written

$$M_x \equiv M_{11} = -D(w_{,xx} + \nu w_{,yy}), \quad M_y \equiv M_{22} = -D(w_{,yy} + \nu w_{,xx}) \tag{20a, b}$$

$$M_{xy} \equiv M_{12} = D(1-\nu)w_{,xy}, \quad M_{yx} \equiv M_{21} = -M_{12} \tag{20c, d}$$

and

$$Y_x \equiv Y_{11} = 2D^l w_{,xy}, \quad Y_y \equiv Y_{22} = -2D^l w_{,xy} \tag{21a, b}$$

$$Y_{xy} \equiv Y_{12} = D^l(w_{,yy} - w_{,xx}), \quad Y_{yx} \equiv Y_{21} = Y_{12} \tag{22c, d}$$

where

$$D = \frac{Eh^3}{12(1-\nu^2)} \tag{23a}$$

is the bending rigidity of the plate and

$$D^l = l^2 Gh = \frac{El^2 h}{2(1+\nu)} \tag{23b}$$

is the contribution of rotation gradients to the bending rigidity. The ratio of the total rigidity $D + D^l$ over the bending rigidity is

$$\frac{D+D^l}{D} = 1 + \frac{D^l}{D} = 1 + 6(1-\nu)\frac{l^2}{h^2} \tag{23c}$$

Substituting Eqs. (14a,b,c) and (15a,b,c) and Eqs. (20) and (21a,b) into Eq. (9), in the absence of body force and body couple, yields

$$\begin{aligned}\delta\Pi = \int_\Omega &[(-M_x - Y_{xy})\delta w_{,xx} + (2M_{xy} + Y_x - Y_y)\delta w_{,xy} \\ &+ (-M_y + Y_{xy})\delta w_{,yy}]d\Omega - \int_\Omega q\delta w d\Omega \\ &+ \int_\Gamma \widetilde{M}_{nn}\delta w_{,n} ds - \int_\Gamma \widetilde{V}_n \delta w ds\end{aligned} \tag{24}$$

which, after the transformation of the domain integral using twice the divergence theorem of Gauss, becomes

$$\begin{aligned}\delta\Pi = -\int_\Omega &[(M_x + Y_{xy})_{,xx} - (2M_{xy} + Y_x - Y_y)_{,xy} \\ &+ (M_y - Y_{xy})_{,yy} + q]\delta w d\Omega - \int_\Gamma \left(M^*_{nn} - \widetilde{M}_{nn}\right)\delta w_{,n} ds \\ &+ \int_\Gamma \left(Q^*_n - \widetilde{V}_n\right)\delta w ds + \int_\Gamma M^*_{nt}\delta w_{,t} ds\end{aligned} \tag{25}$$

where

$$\begin{aligned}Q^*_n = &\left[\frac{\partial}{\partial x}(M_x + Y_{xy}) - \frac{\partial}{\partial y}\left(M_{xy} + \frac{Y_x - Y_y}{2}\right)\right]\cos a \\ &+ \left[\frac{\partial}{\partial y}(M_y - Y_{xy}) - \frac{\partial}{\partial x}\left(M_{xy} + \frac{Y_x - Y_y}{2}\right)\right]\sin a\end{aligned} \tag{26}$$

$$\begin{aligned}M^*_{nn} = &(M_x + Y_{xy})\cos^2 a + (M_y - Y_{xy})\sin^2 a \\ &- 2\left(M_{xy} + \frac{Y_x - Y_y}{2}\right)\cos a \sin a\end{aligned} \tag{27}$$

$$\begin{aligned}M^*_{nt} = &\left(M_{xy} + \frac{Y_x - Y_y}{2}\right)(\cos^2 a - \sin^2 a) + (M_x - M_y + 2Y_{xy}) \\ &\times \cos a \sin a\end{aligned} \tag{28}$$

are the stress resultants and $a = x, \mathbf{n}$. Using Eqs. (20), (21a,b) they become

$$Q^*_n = Q_n + Q^l_n = -(D + D^l)(\nabla^2 w)_{,n} \tag{29}$$

$$M^*_{nn} = M_{nn} + M^l_{nn} = -(D + D^l)(w_{,nn} + \nu w_{,tt}) \tag{30}$$

$$M^*_{nt} = M_{nt} + M^l_{nt} = (D + D^l)(1-\nu)w_{,nt} \tag{31}$$

The above stress resultants consist of two components. The first component is due to pure plate bending and the second one is due to the microstructure plate bending effect.

The last integral in Eq. (25) represents a shearing force term and must be converted in order to be absorbed with the line integral representing potential energy of the shearing force. Noting that $w_{,t} = w_{,s}$ the integration by parts along the boundary Γ of the aforementioned integral gives

$$\begin{aligned}\int_\Gamma M^*_{nt}\delta w_{,s} ds &= \int_\Gamma (M^*_{nt}\delta w)_{,s} ds - \int_\Gamma M^*_{nt,s}\delta w ds \\ &= \sum_k [M^*_{nt}]_k \delta w - \int_\Gamma M^*_{nt,s}\delta w ds\end{aligned} \tag{32}$$

where $[M^*_{nt}]_k$ is the jump of discontinuity of the twisting moment at the k-th corner. Thus, Eq. (25) becomes

$$\begin{aligned}\delta\Pi = -\int_\Omega &[(M_x + Y_{xy})_{,xx} - (2M_{xy} + Y_x - Y_y)_{,xy} \\ &+ (M_y - Y_{xy})_{,yy} + q]\delta w d\Omega - \int_\Gamma \left(M^*_{nn} - \widetilde{M}_{nn}\right)\delta w_{,n} ds \\ &+ \int_\Gamma \left(Q^*_n - M^*_{nt,s} - \widetilde{V}_n\right)\delta w ds + \sum_k [M^*_{nt}]_k \delta w\end{aligned} \tag{33}$$

By applying the principle of total minimum potential energy, i.e., $\delta\Pi = 0$ for the stable equilibrium and the fundamental lemma of the calculus of variation (e.g. Reddy, 1999) the governing equilibrium differential equation of the micro-plate is obtained as

$$(M_x + Y_{xy})_{,xx} - (2M_{xy} + Y_x - Y_y)_{,xy} + (M_y - Y_{xy})_{,yy} + q = 0 \quad \text{in } \Omega \tag{34}$$

together with the boundary conditions

$$Q^*_n - M^*_{nt,s} = \widetilde{V}_n \quad \text{or} \quad w = \tilde{w} \tag{35a}$$

$$M^*_{nn} = \widetilde{M}_{nn} \quad \text{or} \quad w_{,n} = \tilde{w}_{,n} \tag{35b}$$

on Γ and

$$\sum_k [M^*_{nt}]_k = 0 \quad \text{or} \quad w_k = \tilde{w}_k \tag{36}$$

at the k-th corner.

Substituting Eqs. (20) and (21a,b) into Eq. (34) yields the governing equation of the micro-plate in terms of the deflection

$$(D + D^l)\nabla^4 w = q \quad \text{in } \Omega \tag{37}$$

The boundary conditions (35a,b) can be rewritten in the most general form, including elastic support or restraint, as

$$\beta_1 w + \beta_2 V^*_n = \beta_3 \tag{38a}$$

$$\gamma_1 w_{,n} + \gamma_2 M^*_{nn} = \gamma_3 \tag{38b}$$

where β_i, γ_i are functions specified on Γ and

$$V_n^* = V_n + V_n^l = -(D+D^l)\left[(\nabla^2 w)_{,n} - (1-\nu)(w_{,nt})_{,s}\right] \tag{39}$$

is the effective shear force. Note that all conventional boundary conditions can be derived from Eqs. (38) by specifying appropriately the β_i and γ_i. When the boundary Γ is non-smooth the following corner boundary condition must be added to Eqs. (38) (Dym and Shames, 1973)

$$\alpha_{1k} w_k + \alpha_{2k}\left[M_{nt}^*\right]_k = \alpha_{3k}, \quad a_{2k} \neq 0 \tag{40}$$

in which a_{ik} are constants specified at the k-th corner. One can observe that for $l = D^l = 0$ Eqs. (37), (35a,b) and (40) yield the governing equation and the general boundary conditions of the classical plate theory.

In curved boundary the stress resultants M_{nn}^*, V_n^* and M_{nt}^* can be transformed to the local coordinate system of n and s (boundary curvilinear coordinates) using a similar procedure to that for classical plates (Katsikadelis, 1982). That is,

$$M_{nn}^* = -(D+D^l)\left[\nabla^2 w + (\nu-1)(w_{,ss} + \kappa w_{,n})\right] \tag{41}$$

$$V_n^* = -(D+D^l)\left[(\nabla^2 w)_{,n} - (\nu-1)(w_{,sn} - \kappa w_{,s})_{,s}\right] \tag{42}$$

$$M_{nt}^* = (D+D^l)(\nu-1)(w_{,sn} - \kappa w_{,s}) \tag{43}$$

in which $\kappa = \kappa(s)$ is the curvature of the boundary.

Finally, the stress resultants at a point inside Ω are given as

$$M_x^* = -(D+D^l)(w_{,xx} + \nu w_{,yy}), \quad M_y^* = -(D+D^l)(w_{,yy} + \nu w_{,xx}) \tag{44a,b}$$

$$M_{xy}^* = (D+D^l)(1-\nu) w_{,xy} \tag{44c}$$

$$Q_x^* = -(D+D^l)(\nabla^2 w)_{,x}, Q_y^* = -(D+D^l)(\nabla^2 w)_{,y} \tag{45a,b}$$

The solution of Eq. (37) can be written as

$$w = \bar{w} + \hat{w} \tag{46}$$

where $\bar{w}$ is the homogeneous solution and $\hat{w}$ a particular one.

The particular solution is any solution that satisfies only the governing equation independently of the boundary conditions, thus

$$\nabla^4 \hat{w} = q/(D+D^l) \tag{47}$$

There are many techniques to approximate the particular solution when the transverse load q is quite complex. However, when the load is a polynomial of x, y the particular solution can be obtained by transforming Eq. (47) into the complex domain and after successive integrations yields the particular solution. Subsequently, the transformation produces the particular solution in the physical space (Katsikadelis, 2002)

$$\hat{w} = \hat{w}(x, y) \tag{48}$$

The homogeneous solution is obtained from the following boundary value problem

$$(D+D^l)\nabla^4 \bar{w} = 0 \quad \text{in } \Omega \tag{49}$$

and

$$\beta_1 \bar{w} + \beta_2 \overline{V}_n^* = \beta_3 - (\beta_1 \hat{w} + \beta_2 \widehat{V}_n^*) \tag{50a}$$

$$\gamma_1 \bar{w}_{,n} + \gamma_2 \overline{M}_{nn}^* = \gamma_3 - \left(\gamma_1 \hat{w}_{,n} + \gamma_2 \widehat{M}_{nn}^*\right) \tag{50b}$$

on Γ which is solved using the MFS.

4. The method of fundamental solutions

The MFS is considered as a boundary-type meshless method that encompasses all the advantages of the boundary methods such as the BEM unlike the presence of singularities in the fundamental solutions since it is always regular (Zeb et al., 2008). For the problem at hand, both BEM (e.g. Bezine, 1978; Stern, 1979; Katsikadelis and Armenakas, 1989) and MFS (e.g. Karageorghis and Fairweather, 1987; Karageorghis and Fairweather, 1988; Karageorghis and Fairweather, 1989) have been successfully employed to the solution of the biharmonic equation. However, the open issue of the MFS is the location of the source points. Two schemes are referred in the bibliography for the location choice of the source points, the adaptive and the fixed one. In this work the fixed scheme is adopted due to its simple implementation, computational efficiency and convergence proof (Li and Zhu, 2009).

According to MFS, the solution of the boundary value problem described by Eqs. (49) and (50) is approximated as

$$\bar{w}(P) = \sum_{j=1}^{N} c_j G_1(P, Q_j) + \sum_{j=1}^{N} d_j G_2(P, Q_j), \quad P : \{x, y\} \in \Omega \cup \Gamma \tag{51}$$

where c_j and d_j are $2N$ coefficients to be determined; $G_1(P, Q_j), G_2(P, Q_j)$ are the fundamental solutions of the Laplace and the biharmonic operator, respectively, given as

$$G_1(P, Q) = \frac{1}{2\pi} \ln(r_{PQ}), \quad G_2(P, Q) = \frac{1}{8\pi} r_{PQ}^2 \ln(r_{PQ}) \tag{52a,b}$$

and Q_j are N source points distributed appropriately outside of the domain Ω; $r_{PQj} = |P - Q_j|$ is the distance between the point P and the source point Q_j (see Fig. 1).

It is apparent that $\bar{w}(P)$ given by Eq. (49) is a function of x, y. Hence, its derivatives are obtained by direct differentiation. Namely,

$$\bar{w}_{,klmn}(P) = \sum_{j=1}^{N} c_j G_{1,klmn}(P, Q_j) + \sum_{j=1}^{N} d_j G_{2,klmn}(P, Q_j), \quad P : \{x, y\} \in \Omega \cup \Gamma \tag{53}$$

where $k, l, m, n = 0, x, y$. Note that $\bar{w}_{,0000} \equiv \bar{w}$.

The next step of the method is to choose N points – usually distributed uniformly – along the boundary. Eqs. (51) and (53) when applied at the N nodal points on Γ give

$$\bar{\mathbf{w}} = \mathbf{c}\mathbf{G}_1 + \mathbf{d}\mathbf{G}_2 \tag{54}$$

$$\bar{\mathbf{w}}_{,klmn} = \mathbf{c}\mathbf{G}_{1,klmn} + \mathbf{d}\mathbf{G}_{2,klmn}, \quad k, l, m, n = 0, x, y \tag{55}$$

where $\mathbf{G}_1, \mathbf{G}_2, \mathbf{G}_{1,klmn}, \mathbf{G}_{2,klmn}$ are known $N \times N$ matrices originating from the differentiation of the fundamental solutions and their derivatives and $\bar{\mathbf{w}}, \bar{\mathbf{w}}_{,klmn}$ are $N \times 1$ vectors including the homogeneous solution $\bar{w}$ and its derivatives at the N boundary points.

In order to determine the $2N$ unknown coefficients c_j and d_j the homogeneous solution $\bar{w}$ and its derivatives should satisfy the boundary conditions (50) when they also applied at the N nodal points on Γ, thus

$$\mathbf{B}_1 \bar{\mathbf{w}} + \mathbf{B}_2 \overline{\mathbf{V}}_n^* = \mathbf{b}_1 \tag{56a}$$

$$\mathbf{\Gamma}_1 \bar{\mathbf{w}}_{,n} + \mathbf{\Gamma}_2 \overline{\mathbf{M}}_{nn}^* = \mathbf{b}_2 \tag{56b}$$

where $\mathbf{B}_1, \mathbf{B}_2, \mathbf{\Gamma}_1, \mathbf{\Gamma}_2$ are known $N \times N$ diagonal matrices containing the values of $\beta_1, \beta_2, \gamma_1, \gamma_2$ and $\mathbf{b}_1, \mathbf{b}_2$ are known $N \times 1$ vectors.

After the substitution of Eqs. (54) and (55) into Eq. (56) yields a $2N$ linear system of algebraic equations from which the $2N$ unknown values of the coefficients c_j and d_j are determined.

5. Numerical examples

On the base of the procedure described in previous section a FORTRAN program has been written for establishing the bending response of the Kirchhoff micro-plates. In all examples the results have been obtained distributing uniformly the boundary nodes on

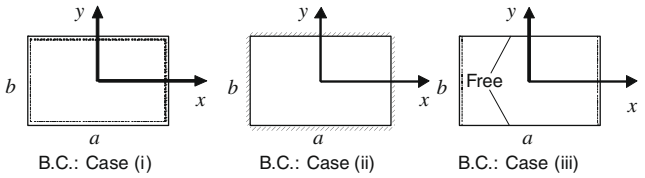

Fig. 2. Boundary conditions of the rectangular micro-plate. Case (i) all edges simply supported, Case (ii) all edges fixed and Case (iii) two opposite edges simply supported and the other two free.

the boundary. The source points are placed equally on a virtual boundary – outside the domain – at a distance 20% greater than that of the actual one.

5.1. Rectangular and elliptical micro-plates

For reasons of comparison both rectangular ($N = 84$) and elliptical ($N = 200$) plates with various aspect ratios are first investigated using the classical Kirchhoff theory ($l = D^l = 0, D = 1$). The employed data are: $q = 1, a = 1, v = 0.30$. Three different cases of boundary conditions are examined for the rectangular plate, namely, (i) all edges simply supported, (ii) all edges clamped and (iii) two opposite edges simply supported and the other two free (see Fig. 2), while the (i) simply supported and (ii) clamped cases are examined for the elliptical plate. In Tables 1 and 2 results for the central deflection and bending moments in rectangular and elliptical plates for three different aspect ratios are presented, which are in excellent agreement as compared with those obtained from the analytical solutions of Timoshenko and Woinowsky-Krieger (1959).

Afterwards, the plate was analyzed taking into account the microstructural effect, as measured by the material length scale parameter $l(D + D^l = 1 + 6(1 - v)(l/h)^2)$. In Fig. 3 the normalized central deflection w_0/w_0^c of both rectangular and elliptical micro-plates versus the square of the non-dimensional material length scale parameter l/h is depicted for three different aspect ratios and Poisson's ratios ($v = 0.25, 0.30, 0.35$) while the aforementioned boundary conditions are considered. From the presented results can be concluded that the deflection of the plate decreases nonlinearly with the increase of l/h. This response presents a similarity to that obtained by Papargyri-Beskou and Beskos (2008) for a square simply supported gradient elastic plate, in which the normalized deflection decreases with increasing the normalized gradient coefficient. From Fig. 3 can also be pointed out that in both rectangular and elliptical micro-plates the rate of decrease of the normalized central deflection depends only on the Poisson's ratio and is totally independent on the boundary conditions and the aspect ratio. That is, for a given Poisson's ratio and external applied lateral load, the normalized deflection is the same for all plates. From the same figure, it is also observed that the deflection of the micro-plates decrease with the increase of the Poisson's ratio.

Table 2
Central deflection and bending moments in the elliptical plate for two cases of boundary conditions and various aspect ratios. Upper row: exact, Lower row: computed.

	B.C.: case(i)			B.C.: case(ii)		
a/b	w^c	M_x^c	M_y^c	w^c	M_x^c	M_y^c
1.0	0.0641	0.2060	0.2060	0.0156	0.0813	0.0813
	0.0637	0.2062	0.2062	0.0156	0.0812	0.0812
1.5	0.0228	0.0987	0.1427	0.0055	0.0369	0.0562
	0.0226	0.0968	0.1423	0.0055	0.0369	0.0562
2.0	0.0090	0.0525	0.0948	0.0021	0.0186	0.0364
	0.0089	0.0512	0.0939	0.0021	0.0186	0.0364

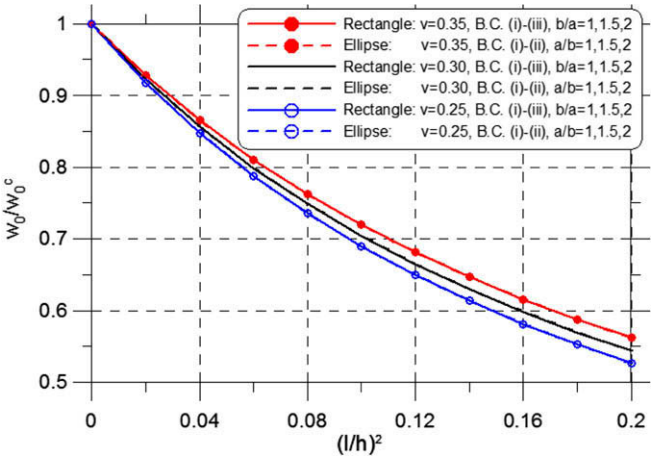

Fig. 3. Normalized central deflection of both rectangular and elliptical micro-plates versus the square of the non-dimensional material length scale parameter for three different aspect ratios and Poisson's ratios.

This was also concluded by Ma et al. (2008) studying the microstructure effect of a simply supported Timoshenko beam model based on the modified couple stress theory of Yang et al. (2002).

Moreover, in Figs. 4–8 the deflection profiles at $y = 0$ for both rectangular ($a/b = 1/1$) and elliptical ($a/b = 0.5/0.63662$) micro-plates are presented for various values of the non-dimensional material length scale parameter l/h, as obtained by the classical Kirchhoff theory and by the proposed plate model ($v = 0.30$). It can be seen that, for all the boundary condition cases, the deflections estimated by the proposed model are always smaller than that by the classical theory. Also, the differences between the two models reduce as the thickness of the plate increases (the ratio l/h decrease) indicating that the size effect is only significant at the micron-scale. To the same conclusion came Park and Gao (2006) and Ma et al. (2008) studying the deflections of a cantilever

Table 1
Central deflection and bending moments in the rectangular plate for three cases of boundary conditions and various aspect ratios. Upper row: exact, lower row: computed.

	B.C.: case(i)			B.C.: case(ii)			B.C.: case(iii)		
b/a	w^c	M_x^c	M_y^c	w^c	M_x^c	M_y^c	w^c	M_x^c	M_y^c
1.0	0.0406	0.0479	0.0479	0.0013	0.0231	0.0231	0.0131	0.1225	0.0271
	0.0406	0.0479	0.0479	0.0013	0.0231	0.0231	0.0131	0.1226	0.0271
1.5	0.0077	0.0812	0.0498	0.0022	0.0368	0.0203	–	–	–
	0.0077	0.0812	0.0498	0.0022	0.0368	0.0203	0.0129	0.1228	0.0339
2.0	0.0101	0.1017	0.0464	0.0025	0.0412	0.0158	0.0128	0.1231	0.0366
	0.0101	0.1016	0.0463	0.0025	0.0412	0.0158	0.0128	0.1233	0.0365

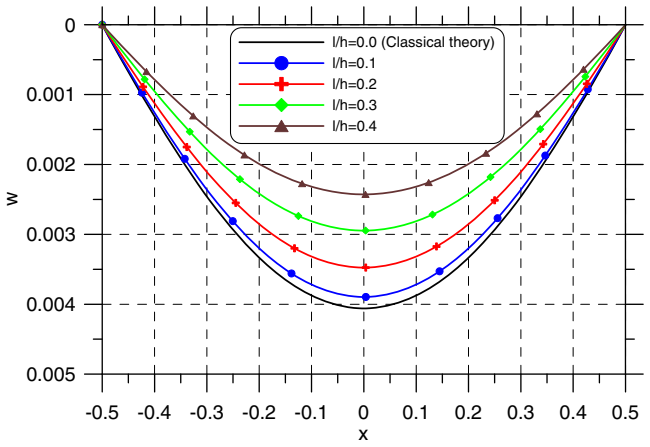

Fig. 4. Deflection profiles at $y = 0$ of the rectangular micro-plate. Boundary conditions: Case (i).

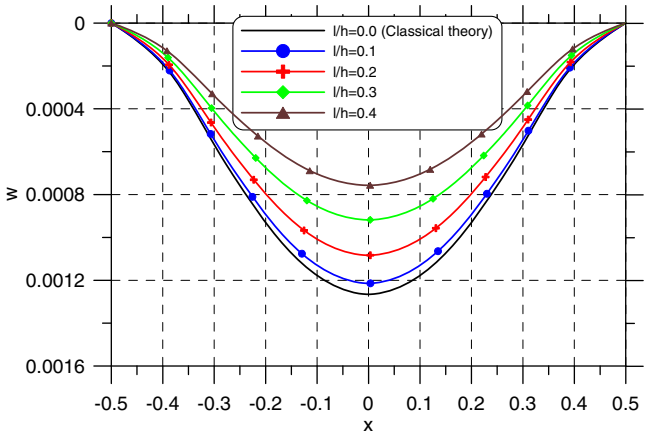

Fig. 5. Deflection profiles at $y = 0$ of the rectangular micro-plate. Boundary conditions: Case (ii).

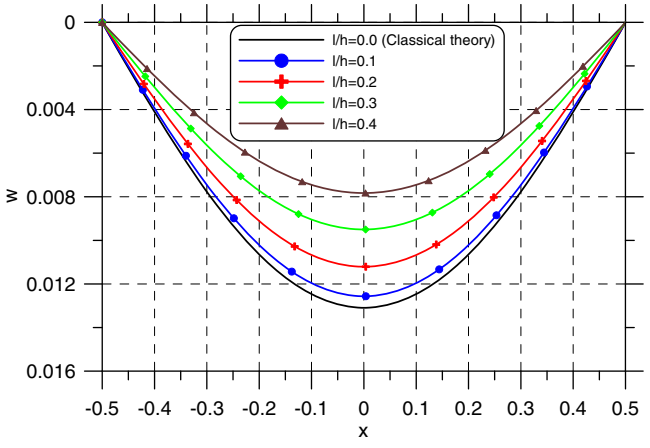

Fig. 6. Deflection profiles at $y = 0$ of the rectangular micro-plate. Boundary conditions: Case (iii).

Bernoulli-Euler beam and a simply supported Timoshenko beam, respectively, using the same modified couple stress theory.

Finally, in order to examine the influence of the micro-plate shape on the deflection and on the stress resultants, the bending

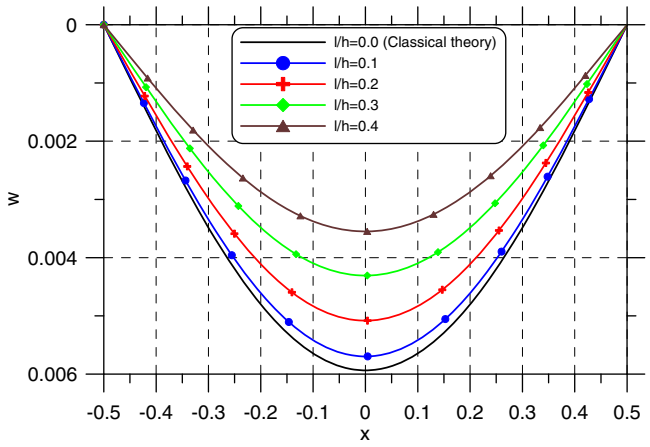

Fig. 7. Deflection profiles at $y = 0$ of the elliptical micro-plate. Boundary conditions: Case (i).

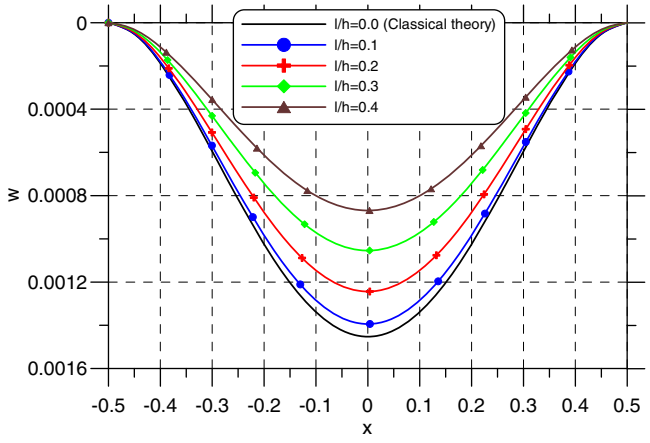

Fig. 8. Deflection profiles at $y = 0$ of the elliptical micro-plate. Boundary conditions: Case (ii).

Table 3
Central deflection and maximum absolute bending moment in the rectangular and elliptical micro-plates ($V = 1, l/h = 0.3$).

	Simply supported		Clamped	
a/b	w_0	$\|M\|_{max}$	w_0	$\|M\|_{max}$
Rectangle: 1/1	0.0030	0.0479	0.00092	0.0506
Ellipse: 0.5/0.63662	0.0043	0.0696	0.00105	0.0465
Rectangle: 1.12838/0.88623	0.0028	0.0395	0.00083	0.0530
Ellipse: 0.56419/0.56419	0.0047	0.0656	0.00115	0.0398
Rectangle: 1.2/0.83333	0.0026	0.0541	0.00074	0.0513
Ellipse: 0.6/0.53052	0.0046	0.0687	0.00112	0.0434

response of a rectangular and of an elliptical micro-plate was investigated keeping fixed the volume of the material V. In Table 3 results for the central deflection and the maximum absolute bending moment are presented for simply supported and clamped micro-plates ($V = 1, l/h = 0.3$). It is obvious that in the simply supported boundary condition case the rectangular micro-plate achieves both smaller deflection and maximum bending moment than the elliptical one. In the clamped boundary condition case only the deflection of the rectangular micro-plate is smaller while the maximum bending moment is always higher than that of the elliptical one.

5.2. Micro-plate with arbitrary shape

In order to demonstrate the capability of the method to treat plates with complex geometries, a simply supported micro-plate with arbitrary shape has been analyzed ($N = 100$). The boundary of the plate is defined by the curve $r = 0.8(|\sin\theta|^3 + |\cos\theta|^3), 0 \leqslant \theta \leqslant 2\pi$. The employed data are: $q = 1, \nu = 0.30$, $D + D^l = 1 + 6(1-\nu)(l/h)^2$ and $l/h = 0.2$. The contours of the deflected surface, the stress resultant M_x^* and the principal stress resultant $M_1^* = \frac{M_x^* + M_y^*}{2} + \sqrt{\left(\frac{M_x^* - M_y^*}{2}\right)^2 + \left(M_{xy}^*\right)^2}$ are depicted in Figs. 9–11, respectively.

6. Conclusions

In this paper a new Kirchhoff plate model was developed for the static analysis of isotropic micro-plates with arbitrary shape containing only one internal material length scale parameter which can capture the size effect. From a detailed variational procedure the governing equilibrium equation and the most general boundary conditions of the micro-plate are derived in terms of the deflection using the principle of minimum potential energy. The resulting boundary value problem is of the fourth order and it is solved using the Method of Fundamental Solutions (MFS). The main conclusions that can be drawn from this investigation are summarized as:

- The present formulation is alleviated from the drawback of existing micro-plate models, the analytic solutions of which are restricted only to micro-plates with simple geometric shapes. That is, the proposed plate model is capable of handling micro-plates with complex geometries and mixed boundary conditions.
- The deflection of the micro-plates decreases nonlinearly with the increase of material length parameter. It depends only on the Poisson's ratio and is totally independent on the boundary conditions and the aspect ratio.
- The increase of the Poisson's ratio produces decrement in the deflection of the micro-plate.

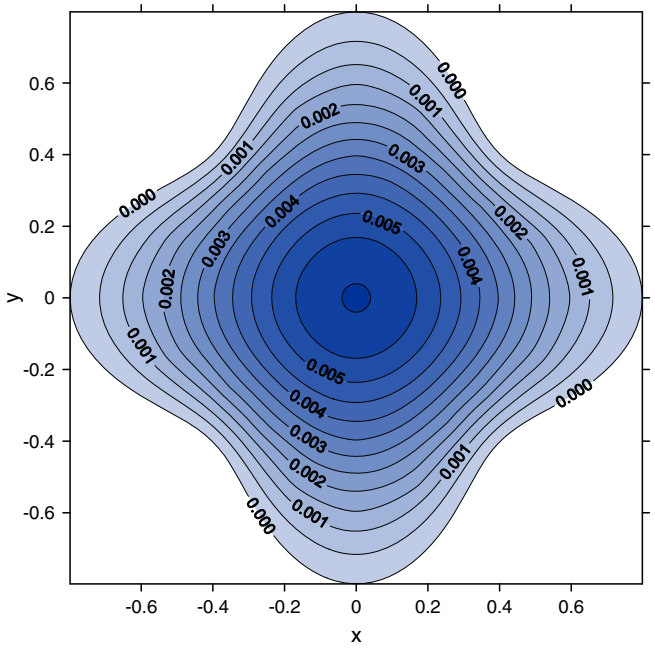

Fig. 9. Contours of the deflected surface in the micro-plate with arbitrary shape.

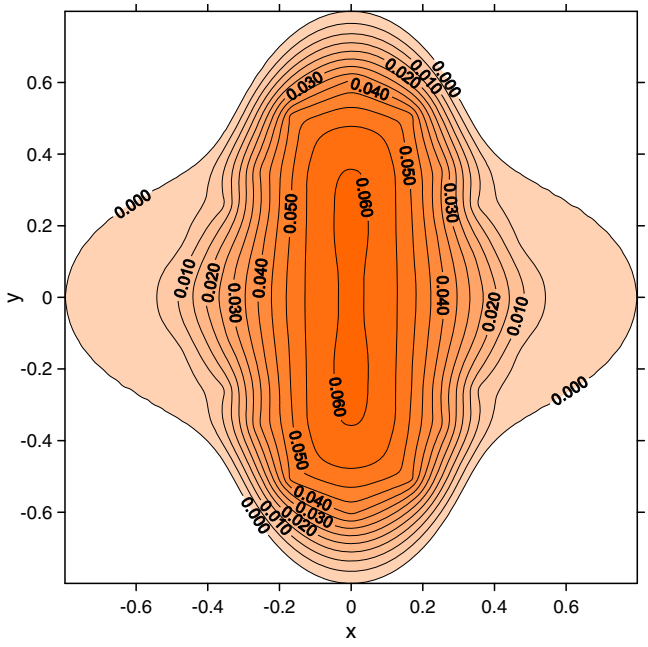

Fig. 10. Contours of the stress resultant M_x^* in the micro-plate with arbitrary shape.

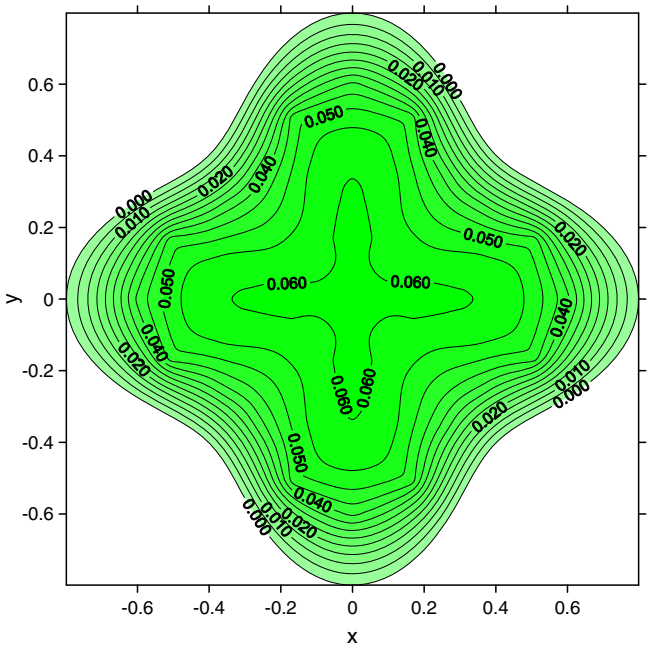

Fig. 11. Contours of the principal stress resultant M_1^* in the micro-plate with arbitrary shape.

- For all the examined boundary condition cases, the deflection estimated by the proposed model is always smaller than that by the classical theory.
- The difference of the results obtained by the two models (present and classical) reduces as the thickness of the plate increases (the ratio l/h decrease) indicating that the size effect is only significant at the micron-scale.
- For rectangular and elliptical micro-plates with fixed material volume it is proved that in the simply supported boundary condition case the rectangular micro-plate achieves both smaller deflection and maximum bending moment than the elliptical

one. In the clamped boundary condition case only the deflection of the rectangular micro-plate is smaller while the maximum bending moment is always higher than that of the elliptical one.

References

Altan, B.S., Aifantis, E.C., 1992. On the structure of the mode III crack-tip in gradient elasticity. Scripta Met. 26, 319–324.

Askes, H., Aifantis, E.C., 2002. Numerical modeling of size effects with gradient elasticity – Formulation, meshless discretization and example. Int. J. Fracture 117, 347–358.

Bezine, G., 1978. Boundary integral equations for plate flexure with arbitrary boundary conditions. Mech. Res. Commun. 5, 197–206.

Dym, C.L., Shames, J.H., 1973. Solid mechanics. A variational approach. McGraw-Hill, New York.

Exadaktylos, G.E., Vardoulakis, I., 2001. Microstructure in linear elasticity and scale effects: a reconsideration of basic rock mechanics and rock fracture mechanics. Tectonophysics 335, 81–109.

Gao, X.-L., Park, S.K., 2007. Variational formulation of a simplified strain gradient elasticity theory and its application to a pressurized thick-walled cylinder problem. Int. J. Solids Struct. 44, 7486–7499.

Karageorghis, A., Fairweather, G., 1987. The method of fundamental solutions for the numerical solution of the biharmonic equation. J. Comput. Phys. 69, 434–459.

Karageorghis, A., Fairweather, G., 1988. The Almansi method of fundamental solutions for solving biharmonic problems. Int. J. Numer. Meth. Eng. 26, 1665–1682.

Karageorghis, A., Fairweather, G., 1989. The simple layer potential method of fundamental solutions for certain biharmonic problems. Int. J. Numer. Meth. Fluids 9, 1221–1234.

Katsikadelis, J.T., 1982. The analysis of plates on elastic foundation by the boundary integral equation method. Ph. D. Thesis, Polytechnic Institute of New York.

Katsikadelis, J.T., 2002. Boundary Elements: Theory and Applications. Elsevier, Amsterdam-London.

Katsikadelis, J.T., Armenakas, A.E., 1989. New boundary equation solution to the plate problem. J. Appl. Mech.-T. ASME 56, 364–374.

Kong, S., Zhou, S., Nie, Z., Wang, K., 2008. The size-dependent natural frequency of Bernoulli–Euler micro-beams. Int. J. Eng. Sci. 46, 427–437.

Koiter, W.T., 1964. Couple stresses in the theory of elasticity, I and II. In: Proc. K. Ned. Akad. Wet. (B) 67, pp. 17–44.

Lam, D.C.C., Yang, F., Chong, A.C.M., Wang, J., Tong, P., 2003. Experiments and theory in strain gradient elasticity. J. Mech. Phys. Solids 51, 1477–1508.

Lazopoulos, K.A., 2004. On the gradient strain elasticity theory of plates. Euro. J. Mech. A/Solids 23, 843–852.

Li, X., Zhu, J., 2009. The method of fundamental solutions for nonlinear elliptic problems. Eng. Anal. Bound. Elem. 33, 322–329.

Ma, H.M., Gao, X.-L., Reddy, J.N., 2008. A microstructure-dependent Timoshenko beam model based on a modified couple stress theory. J. Mech. Phys. Solids 56, 3379–3391.

Mindlin, R.D., 1964. Micro-structure in linear elasticity. Arch. Ration. Mech. Anal. 16, 51–78.

Papargyri-Beskou, S., Beskos, D.E., 2008. Static, stability and dynamic analysis of gradient elastic flexural Kirchhoff plates. Arch. Appl. Mech. 78, 625–635.

Park, S.K., Gao, X.-L., 2006. Bernoulli–Euler beam model based on a modified couple stress theory. J. Micromech. Microeng. 16, 2355–2359.

Park, S.K., Gao, X.-L., 2008. Variational formulation of a modified couple stress theory and its application to a simple shear problem. Z. Angew. Math. Phys. 59, 904–917.

Reddy, J.N., 1999. Theory and Analysis of Elastic Plates. Taylor and Francis, Philadelphia.

Stern, M., 1979. A general boundary integral formulation for the numerical solution of plate bending problems. Int. J. Solids Struct. 15, 769–782.

Timoshenko, S.P., Woinowsky-Krieger, S., 1959. Theory of Plates and Shells. McGraw-Hill, New York.

Timoshenko, S.P., Goodier, J.N., 1970. Theory of Elasticity. McGraw-Hill, New York.

Tsepoura, K., Papargyri-Beskou, S., Polyzos, D., Beskos, D.E., 2002. Static and dynamic analysis of gradient elastic bars in tension. Arch. Appl. Mech. 72, 483–497.

Vardoulakis, I., Sulem, J., 1995. Bifurcation Analysis in Geomechanics. Blackie/Chapman and Hall, London.

Yang, F., Chong, A.C.M., Lam, D.C.C., Tong, P., 2002. Couple stress based strain gradient theory of elasticity. Int. J. Solids Struct. 39, 2731–2743.

Zeb, A., Ingham, D.B., Lesnic, D., 2008. The method of fundamental solutions for a biharmonic inverse boundary determination problem. Comp. Mech. 42, 371–379.